NASA Technical Memorandum 110291

A Benchmark Problem For Development of Autonomous Structural Modal Indentification

Richard S. Pappa, Stanley E. Woodard, and Jer-Nan Juang
Langley Research Center, Hampton, Virginia

October 1996

National Aeronautics and
Space Administration
Langley Research Center
Hampton, Virginia 23681-0001

A BENCHMARK PROBLEM FOR DEVELOPMENT OF AUTONOMOUS STRUCTURAL MODAL IDENTIFICATION

Richard S. Pappa, Stanley E. Woodard, and Jer-Nan Juang
NASA Langley Research Center
Hampton, VA 23681

ABSTRACT

This paper summarizes modal identification results obtained using an autonomous version of the Eigensystem Realization Algorithm on a dynamically complex, laboratory structure. The benchmark problem uses 48 of 768 free-decay responses measured in a complete modal survey test. The true modal parameters of the structure are well known from two previous, independent investigations. Without user involvement, the autonomous data analysis identified 24 of 33 structural modes with good to excellent accuracy in 62 seconds of CPU time (on a DEC Alpha 4000 computer). The modal identification technique described in the paper is the baseline algorithm for NASA's Autonomous Dynamics Determination (ADD) experiment scheduled to fly on International Space Station assembly flights in 1997-1999.

INTRODUCTION

Increased miniaturization of computer hardware and sensors, as well as many-fold improvements in their performance, allow new possibilities in the design of spacecraft. Prominent among these is the possibility of increased autonomy. Unexpected events during operation that once required a team of experts to diagnose and fix can conceivably be handled on-board the spacecraft. In the limit, a simple "green light" condition would occur while the spacecraft is operating normally. A "yellow light" would indicate an abnormal condition handled by the flight computers. Upon resolution, a simple text file summarizing the chain of events would be down loaded. A "red light" would indicate an unresolved event (Refs. 1-2).

Autonomy can drastically reduce the size of ground support teams. For example, the recently proposed Pluto Express deep-space mission may require only 10 ground personnel compared with about 200 people for the current Galileo mission to Jupiter (Ref. 1). Power and communications resources on the vehicle are also reduced by minimizing transmission of raw data to Earth. Rather than sending raw data, only the "answers" will be returned. Furthermore, better performance and survivability of the spacecraft is indicated in situations where rapid action is necessary.

Modal parameter identification is the process of calculating natural vibration frequencies, mode shapes, and damping of structures from experimental measurements. Modal parameters are used in many ways. The predominant use in aerospace applications is verification and refinement of finite-element models. Other uses include "trouble-shooting" unexpected vibrations or interactions, adjustment of active control systems, fatigue prediction, and damage detection and resolution. All of these areas are potential uses of autonomous modal identification of spacecraft, with primary emphasis currently given to damage detection and resolution (Ref. 3).

In the majority of laboratory modal tests, the measurements are frequency response functions (FRFs) between one or more excitation sources and a set of accelerometers. Modal parameters are estimated from the FRFs using various time- and/or frequency-domain methods (Ref. 4). In-space applications, however, have traditionally used free-decay responses instead of FRFs in order to minimize data acquisition time and to avoid having to measure excitation forces (Refs. 5,6). References 7 and 8 discuss some of the practical aspects and challenges of in-space data acquisition and structural modal identification.

Autonomous structural modal identification of spacecraft is a new technical subject. The approach given in this paper is a fairly straightforward extension of the Eigensystem Realization Algorithm (ERA), a time-domain identification technique that has evolved over the past decade (Refs. 9-12). More advanced features are being considered (including fuzzy logic, neural networks, and recursive correlation calculations) but are not discussed here. The results presented in this paper for the benchmark problem serve as a standard against which future improvements in modal-identification performance can be gauged.

The next two sections of the paper describe the test article and test procedure, and summarize results of a complete modal survey test using 16 excitation locations and 48 accelerometers. The following section describes the benchmark problem in which 4 of the excitation locations and 12 of the accelerometers are selected. The selections are based on a reasonable approximation of the type of data expected to be obtained in initial flights of NASA's Autonomous Dynamics Determination experiment (ADD). The final two sections of the paper summarize the current autonomous algorithm and present results obtained for the benchmark problem.

TEST ARTICLE AND TEST PROCEDURE

Figure 1 shows the laboratory test structure for this project. It consists of a vertical steel tube and 4 rectangular steel beams of various lengths. The beams are clamped at their centers to the tip and middle of the tube. The upper pair of beams is rotated 45 degrees with respect to the lower pair. One beam of each pair contains a silicon layer at its neutral axis that provides considerable additional damping. The overall dimensions are 63 inches in height and 55 inches in width, and the total mass is approximately 110 lbs. The structure is clamped at its base to a massive seismic block.

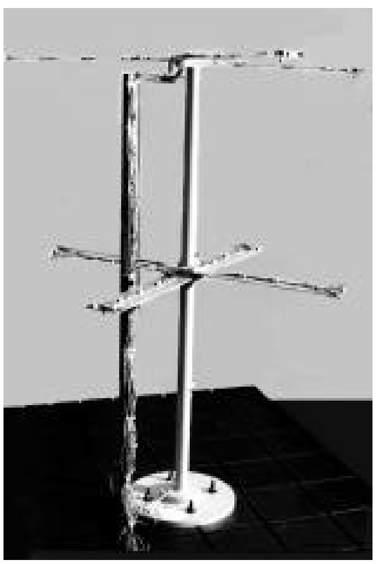

Fig. 1 - Test Structure

This structure was tested in 1991 at the German Aerospace Research Establishment (DLR) in Göttingen, Germany under a collaborative NASA-DLR research program (Refs. 7,13). The data set was selected as a benchmark problem for autonomous algorithm development for the following reasons: 1) a large set of free-decay responses (rather than FRFs) were measured, 2) the structure has dynamically complex properties representative of actual spacecraft characteristics (including modal clusters, wide variation of modal damping, both local and global modes, and moderate nonlinearity), and 3) the true modal parameters are well known based on good correlation of two previous, independent investigations (Ref. 13).

Figure 2 shows the 16 excitation and 48 accelerometer degrees-of-freedom used in the complete modal survey test. This large number of excitations and responses is more than adequate to identify the low-frequency (< 100 Hz) vibration modes of the structure. An impact hammer excited the structure at each excitation point individually. A force measurement on the hammer triggered the data acquisition process, but the force signal itself was not recorded. The data acquisition system recorded free-decay time histories for all 48 responses simultaneously at a sampling rate of 200 Hz for approximately 5 secs.

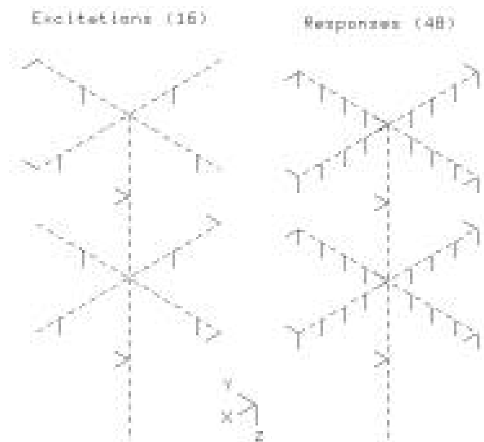

Fig. 2 - Excitations and Responses for Complete Modal Survey

Figure 3 is a typical response measurement and its frequency spectrum. Counting the number of peaks in the spectrum, there appears to be about 10 modes in the 0 to 100 Hz bandwidth. In fact, there are 33 modes. Most measurements from this test article also have less than 10 peaks in their spectrum due to significant modal clustering and local response behavior of many of the modes.

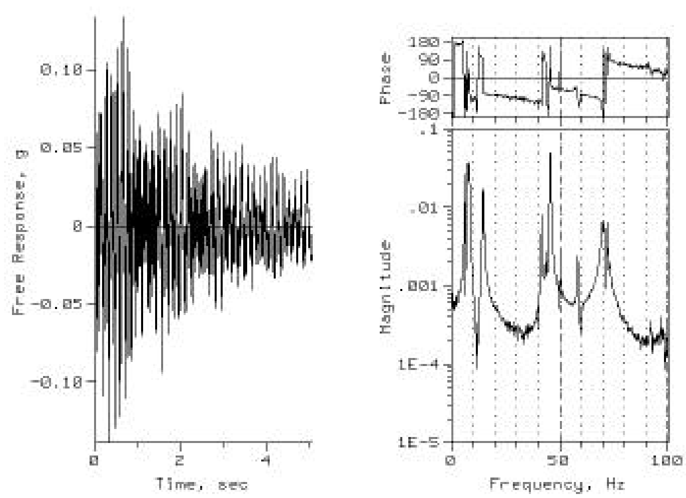

Fig. 3 - Typical Free-Decay Response and Spectrum

MODAL SURVEY RESULTS

This section of the paper summarizes results of the complete modal survey test. These data were analyzed initially in 1991, and the results were compared with those from an entirely different test performed using sine dwell excitation of each mode individually. The two sets of results agreed closely as reported in Ref. 13. At that time, 30 modes were obtained. Additional data analyses since 1991 have improved these results, resulting in identification of 2 additional structural modes. There is also 1 “mode” in the data set at 50 Hz and 0% damping corresponding to the European electrical noise component. This “mode” is included in the results of this paper for completeness in order to fully document the modal identification results for the benchmark problem.

Figure 4 shows the identified natural frequencies, damping factors, and Consistent-Mode Indicator (CMI) values (Ref. 11) for each of the 33 modes. CMI is the primary accuracy indicator of ERA, and ranges in value from 0 to 100%. Modes with CMI values greater than approximately 80% are identified with high confidence. Modes with values from approximately 80% to 1% have moderate to large uncertainty. Fictitious “computational modes” have CMI values of approximately zero.

The frequency results in Fig. 4 clearly show that the modes are primarily clustered in 5 separate bands. Such high modal density (> 1 mode per Hz) makes it impossible to identify all modes with a single excitation. Many modes are weakly excited in each test (characteristic of most complex structures) so it is imperative to correctly separate valid structural modes from extraneous computational modes (also known as “noise modes”).

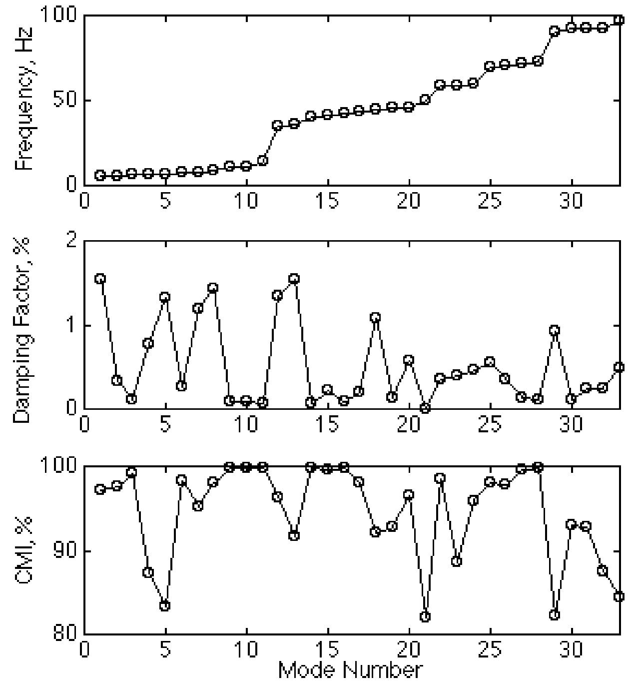

Fig. 4 - Results of Complete Modal Survey

Figure 5 shows example mode shapes from the complete modal survey test. Figure 5(a) is an antisymmetric bending mode of an upper beam. This particular beam contains a silicon layer at its neutral axis which significantly increases damping. The modal damping (ζ) is 1.5% compared with 0.3% for a similar mode of the other upper beam at 5.79 Hz shown in Fig. 5(b). The mode in Fig. 5(b) is also more highly coupled with bending of the vertical mast and lower beams. Figure 5(c) shows the 1st torsion mode which has almost zero damping since only the steel center mast of the structure deforms. Figure 5(d) is a complex, coupled system mode with motion throughout the structure. Its shape is highly nonintuitive.

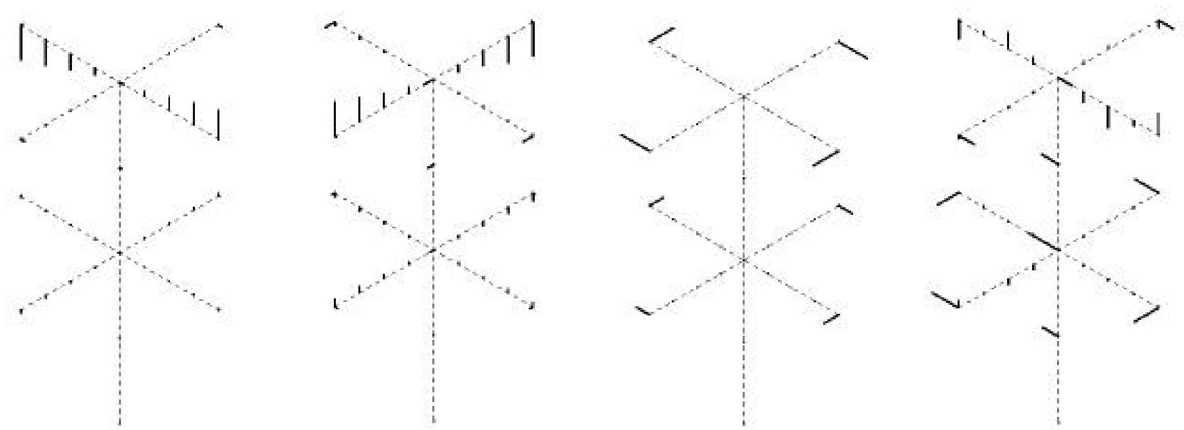

(a) 5.48 Hz (ζ = 1.5%) (b) 5.79 Hz (ζ = 0.3%) (c) 14.37 Hz (ζ = 0.06%) (d) 43.61 Hz (ζ = 0.2%)

Fig. 5 - Example Mode Shapes

The modal identification results for the complete modal survey test are also tabulated near the end of the paper in Table 1. They will be compared at that time with results obtained for the benchmark problem.

BENCHMARK PROBLEM

As an approximation of the data expected to be measured in initial flight applications of autonomous modal identification, the benchmark problem uses a small subset of the 768 measurements from the complete modal survey test. Figure 6 shows the 4 excitation and 12 response degrees-of-freedom selected for the benchmark problem. Excitation points consist of x and z excitation near the tips of one of the upper beams, and x and y excitation of the vertical mast midway between the two pairs of cross beams. Responses consist of 4 measurements in each of the x, y, and z directions distributed on the upper and lower beams and vertical mast.

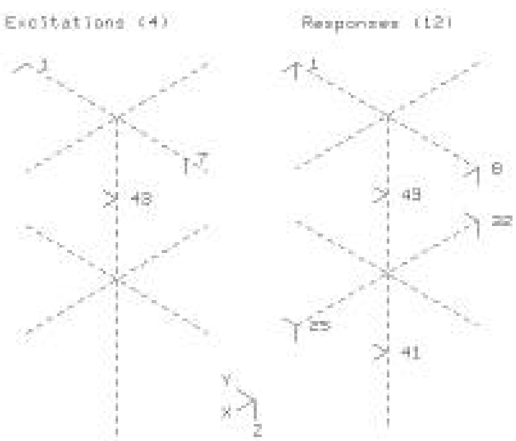

Fig. 6 - Excitations and Responses for Benchmark Problem (Subset of Fig. 2)

Before presenting the results obtained for the benchmark problem using the autonomous modal identification algorithm, the following report section summarizes the procedure.

AUTONOMOUS MODAL IDENTIFICATION ALGORITHM

As mentioned before, the approach given in this paper is a fairly straightforward extension of the Eigensystem Realization Algorithm (ERA) (Refs. 9-12). Other features are being considered including fuzzy logic, neural networks, and recursive correlation analysis, but are not discussed here. Also, the precise steps and parameters may vary for other test articles.

Figure 7 is an overall flowchart of the algorithm. Beginning at the top of the diagram, the 12 responses for Test 1 (Excitation at location 1X) are processed in a single-input, multiple-output (SIMO) ERA analysis with a Hankel matrix size of 300 rows x 100 columns. Every ERA analysis uses this matrix size to simplify implementation. Each analysis also uses automatic singular-value truncation based on a specified root-mean-square measurement noise level. ERA calculates several "accuracy indicators" (Ref. 12, pp. 52-63) in addition to natural frequencies, damping factors, and mode shapes. The primary accuracy indicator is the Consistent-Mode Indicator (CMI) (Ref. 11) which ranges from 0 to 100%. The third block of Fig. 7 deletes modes having CMI less than 50%, damping factors outside the range of 0-30%, or frequencies within 1% of the edges of the analysis bandwidth.

The next step, mode condensation, is a principal autonomous aspect of the procedure. This step is responsible for selecting the best estimate among multiple estimates of the same mode. (Mode condensation becomes more significant as additional sets of results are generated.) Figure 8 describes the mode condensation step in detail. The final set of structural modal parameters (at any point in time) is the last-computed output of the mode condensation process.

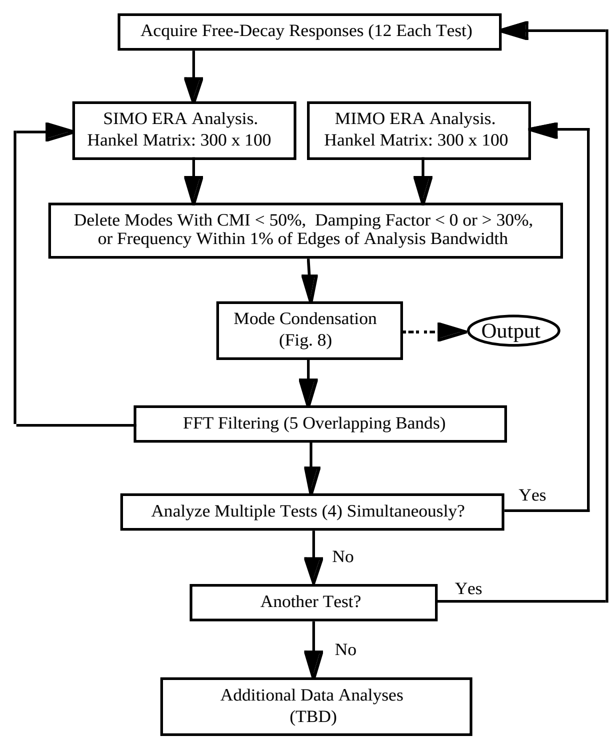

Fig. 7 - Flow Chart of Autonomous Algorithm

- Condensation combines 2 sets of identified modal parameters: a new set, Set 1, and an old set, Set 2. (Set 2 is the final, condensed set.)
- Compare each frequency in Set 1 with those in Set 2. If there are no frequencies in Set 2 within 10% of the frequency of Mode n in Set 1, add Mode n to Set 2.
- If there are one or more modes in Set 2 within 10% of the frequency of Mode n, calculate the Modal Assurance Criterion (MAC) (Ref. 12, p. 113) between each of these pairs of modes.
  - If all MAC's are less than 70%, add Mode n to Set 2.
  - Otherwise, select the mode from Set 2 having the highest MAC with Mode n. If the CMI of this mode is less than the CMI of Mode n, replace the mode in Set 2 with Mode n from Set 1.

Fig. 8 - Mode Condensation

Following mode condensation, the data are filtered by fast Fourier transformation, selection of a specified frequency range, then inverse fast Fourier transformation (Ref. 14, p. 195). This is a highly effective and efficient filtering method for transient data. The benchmark problem uses five overlapping bands, in addition to a baseband analysis without filtering, as shown in Fig. 9. The number of data points in each filter band is always a power of 2 for maximum FFT speed.

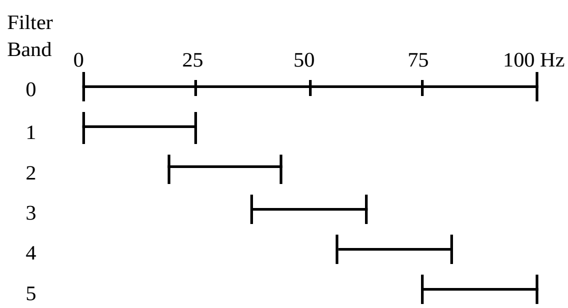

Fig. 9 - Filter Bands

After filtering, the next step in Fig. 7 is a decision concerning the analysis of multiple tests simultaneously. ERA is a multiple-input, multiple-output (MIMO) time domain technique that is normally used in a MIMO fashion. However, for in-space applications requiring minimum computer memories (as well as probably no disk drive), it may be impractical to perform MIMO analyses. Furthermore, because the response data for each test are acquired separately (perhaps at widely spaced time intervals), they may not be "consistent" enough for MIMO analysis. Consistent data in modal testing refers to data sets with identical modal parameters. Consistency is difficult to achieve with practical structures (due to nonlinearity and/or nonstationarity) when data sets are acquired in separate tests. In laboratory tests, data (FRFs) are usually measured using multiple-input random excitation to minimize inconsistencies.

For the benchmark problem, a MIMO analysis is performed after each of the 4 data sets is analyzed individually. For in-space implementation, a different strategy than this may be used. For example, MIMO analyses may be performed on every 2 or 3 data sets in a "sliding" manner. As shown in the final block of Fig. 7, other types of data analyses (e.g., using "key data" to enhance individual modes of interest, Ref. 12, p. 168) may also occur in flight applications as time permits.

Figure 10 shows the cases run on the benchmark problem using the autonomous algorithm. Test Numbers 1-4 are SIMO analyses of data sets for excitations 1X, 7Z, 43X, and 43Y, respectively. Test No. 5 is a MIMO analysis using all 4 data sets simultaneously. Each of the 5 tests uses 6 different filter bands (shown in Fig. 9) for a total of 30 cases.

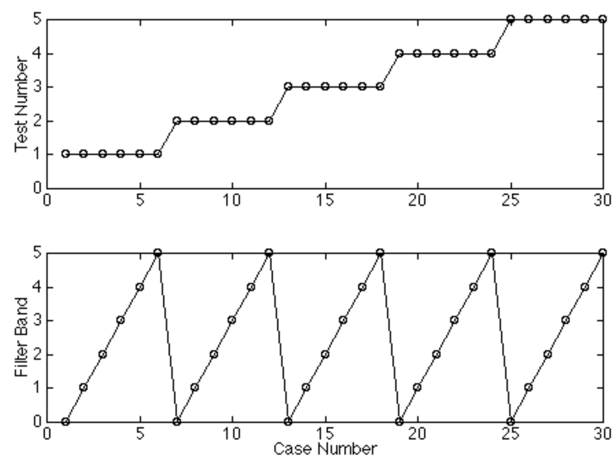

Fig. 10 - Cases Run on Benchmark Problem

BENCHMARK PROBLEM RESULTS

Figure 11 and Table 1 summarize the modal identification results for the benchmark problem using autonomous modal identification as described in the previous section. Figure 11 shows the number of identified modes versus case number. These results are the output of the mode condensation process at the end of each case. Drops in the results indicate replaced modes according to the logic described in Fig. 8. The 30 cases ran sequentially without user involvement. The total execution CPU time was 62 seconds on a DEC Alpha 4000 computer using a FORTRAN implementation.

Recall from Fig. 10 that Case Numbers 1-24 are SIMO analyses while Case Numbers 25-30 are MIMO analyses. Figure 11 shows that the MIMO analyses made only a small improvement in the number of identified modes (5 modes replaced). The largest change in number of identified modes occurred in Cases 1, 7, and 19 which are baseband analyses (no filtering), and in Case 2 which is analysis of the 1X data set using 0-25 Hz filtering. Of course, it becomes increasingly more difficult to make significant changes in the overall set of results as the total

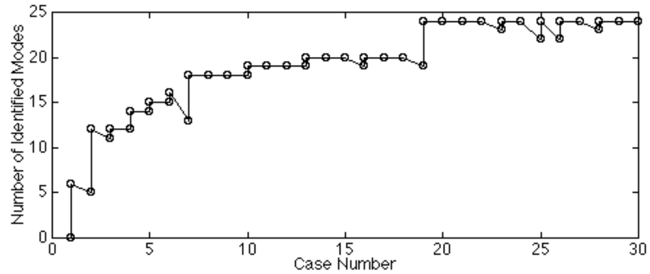

Fig. 11 - No. of Identified Modes vs. Case No. (Drops Indicate Replaced Modes)

Benchmark Problem Results Using Autonomous Algorithm				Complete Modal Survey Results			Mode Shape Correlation
Mode No.	Frequency, Hz	Damping Factor, %	CMI, %	Frequency, Hz	Damping Factor, %	CMI, %	MAC, %
1	5.521	1.456	93.84	5.483	1.545	97.12	99.93
2	5.781	0.304	91.27	5.788	0.337	97.59	99.52
				6.668	0.114	99.18	-
3	6.664	1.319	73.91	6.784	0.768	87.21	98.41
4	6.701	2.333	86.13	6.864	1.315	83.27	93.08
5	7.215	0.175	91.74	7.227	0.258	98.17	99.86
6	8.021	1.316	86.70	8.020	1.179	95.27	99.54
				9.052	1.433	98.09	-
				11.254	0.094	99.72	-
7	11.375	0.266	82.40	11.393	0.086	99.71	99.08
8	14.374	0.057	99.65	14.374	0.058	99.83	100.00
9	34.456	1.413	75.58	34.352	1.345	96.29	99.98
10	36.092	1.526	84.47	36.111	1.540	91.71	99.99
11	39.900	0.072	99.11	39.899	0.071	99.82	99.99
12	41.514	0.232	98.78	41.507	0.226	99.57	99.94
				42.374	0.087	99.75	-
13	43.601	0.212	96.35	43.605	0.199	98.02	99.98
				43.933	1.074	92.04	-
14	45.695	0.134	75.33	45.694	0.133	92.76	99.98
15	46.199	0.921	51.43	46.122	0.564	96.38	87.49
16 †	49.982	0.004	72.76	49.994	0.001	82.07	55.57
17	58.225	0.343	96.45	58.225	0.361	98.54	99.57
				58.699	0.399	88.65	-
18	59.201	0.538	90.62	59.299	0.471	95.90	98.85
19	69.755	0.560	74.07	69.647	0.539	98.12	90.55
20	70.254	0.103	50.85	70.377	0.348	97.85	85.29
21	71.705	0.112	89.89	71.700	0.131	99.60	99.79
				72.747	0.112	99.77	-
22	90.958	0.678	69.32	90.743	0.913	82.10	93.99
23	92.008	0.520	54.77	92.054	0.112	92.91	93.87
				92.626	0.239	92.71	-
24	92.293	0.797	80.17	92.674	0.244	87.41	89.94
				97.269	0.487	84.44	-

† Electrical Noise (Europe)

Table 1 - Benchmark Problem Results and Comparison With Complete Modal Survey Test

number of cases increases.

Table 1 tabulates the final results of the benchmark problem. A total of 24 modes are identified compared with 33 found in the complete modal survey test (including the fictitious “mode” at 50 Hz due to electrical noise). Each mode of the benchmark problem is aligned in the table with its corresponding mode from the complete modal survey. The righthand column shows the Modal Assurance Criterion (MAC) value (correlation coefficient) between the two sets of mode shapes at the 12 response locations common to both sets. Overall accuracy of the benchmark problem is good to excellent based on the distribution of CMI values which is as follows: 9 modes have CMI values greater than 90%, 6 additional modes have CMI values between 80% and 90%, and the remaining CMI values are less than 80%. A CMI threshold of 80% has traditionally been used as the lower boundary of modal parameters identified with “high” confidence.

CONCLUSIONS

The research reported in this paper contributes to the development of more-autonomous future spacecraft. In particular, the autonomous modal identification technique described in the paper will serve as the baseline algorithm for NASA’s Autonomous Dynamics Determination (ADD) experiment scheduled to fly on International Space Station assembly flights in 1997-1999. The results of the benchmark problem are a standard against which the effectiveness of algorithm modifications can be judged. The benchmark problem used a dynamically complex laboratory structure with characteristics typical of operating spacecraft including modal clusters and both local and global modes. For application to specific spacecraft structures, the parameters in the procedure will be “tuned” based on problem-specific results obtained using finite-element model simulations.

REFERENCES

1. Iannotta, B., “NASA Officials Weigh Pluto Mission Request,” *Space News*, Nov. 27-Dec. 3, 1995, pp. 4, 21.

2. Ferster, W., “NASA Sets Big Goals for Miniature Spacecraft Series,” *Space News*, May 20-26, 1996, p. 9.

3. Zimmerman, D. C., Smith, S. W., Kim, H.-M., and Bartkowicz, T. J., “Spacecraft Applications for Damage Detection Using Vibration Testing,” *Proceedings of the 14th IMAC*, Feb. 1996, pp. 851-856.

4. Allemang, R. J. and Brown, D. L., “Experimental Modal Analysis," Chapter 21 in *Shock and Vibration Handbook*, Harris, C. M. and Crede, C. E., editors, Fourth Edition, McGraw-Hill Book Company, 1995.

5. Blelloch, P., Engelhardt, C., and Hunt, D. L., “Simulation of On-Orbit Modal Tests of Large Space Structures,” *Proceedings of the 8th IMAC*, Jan. 1990, pp. 926-932.

6. Gilbert, M. G. and Welch, S. S., “STS-74/MIR Photogrammetric Appendage Structural Dynamics Experiment,” *Proceedings of AIAA Structures, Structural Dynamics, and Materials Conference*, 1996.

7. Schenk, A. and Pappa, R. S., "Practical Aspects of On-Orbit Modal Identification Using Free-Decay Data," *Journal of Spacecraft and Rockets*, Vol. 29, No. 2, March-April 1992, pp. 264-270.

8. Pappa, R. S., "Identification Challenges for Large Space Structures," *Sound and Vibration*, April 1990, pp. 16-21.

9. Juang, J.-N. and Pappa, R. S., "An Eigensystem Realization Algorithm for Modal Parameter Identification and Model Reduction," *Journal of Guidance, Control, and Dynamics*, Vol. 8, No. 5, Sept.-Oct. 1985, pp. 620-627.

10. Juang, J.-N., Horta, L. G., and Phan, M., "System/Observer/Controller Identification Toolbox,” NASA TM-107566, Feb. 1992.

11. Pappa, R. S., Elliott, K. B., and Schenk, A., "Consistent-Mode Indicator for the Eigensystem Realization Algorithm," *Journal of Guidance, Control, and Dynamics*, Vol. 16, No. 5, Sept.-Oct. 1993, pp. 852-858.

12. Pappa, R. S., “Eigensystem Realization Algorithm User's Guide for VAX/VMS Computers,” NASA TM-109066, May 1994.

13. Pappa, R. S., Schenk, A., Niedbal, N., and Klusowski, E., "Comparison of Two Dissimilar Modal Identification Techniques," *Journal of Guidance, Control, and Dynamics*, Vol. 15, No. 4, July-Aug. 1992, pp. 840-846.

14. Hamming, R. W., *Digital Filters*, Second Edition, Prentice-Hall, Inc., 1983.